ADVANCED FUNCTIONAL MATERIALS

Supporting Information

for *Adv. Funct. Mater.*, DOI 10.1002/adfm.202310133

Bulk In Situ Reconstruction of Heterojunction Perovskite Enabling Stable Solar Cells Over 24% Efficiency

Shanyue Hou, Zhu Ma, Yanlin Li, Zhuowei Du, Yi Chen, Junbo Yang, Wei You, Qiang Yang, Tangjie Yu, Zhangfeng Huang, Guomin Li, Haoyu Wang, Qianyu Liu, Guangyuan Yan, Haimin Li*, Yuelong Huang*, Wenhua Zhang*, Mojtaba Abdi-Jalebi*, Zeping Ou, Kuan Sun, Rong Su and Wei Long*

Bulk in-situ reconstruction of heterojunction perovskite enabling stable solar cells over 24% efficiency

Shanyue Hou[1], Zhu Ma[1]*, Yanlin Li[1], Zhuowei Du[1], Yi Chen[1], Junbo Yang[1], Wei You[1], Qiang Yang[1], Tangjie Yu[1], Zhangfeng Huang[1], Guomin li[1], Haoyu Wang[1], Qianyu Liu[1], Guangyuan Yan[1], Haimin Li[1]*, Yuelong Huang[1, 2]*, Wenhua Zhang[3]*, Mojtaba Abdi Jalebi[4]*, Zeping Ou[5], Kuan Sun[5], Rong Su[6], Wei Long[6]

Support information

Experimental section

Materials

SnO_2 (15% in H_2O colloidal dispersion) was purchased from Alfa Aesar. Dimethyl sulfoxide (DMSO, anhydrous, ≥99.9%), N, N-dimethylformamide (DMF, anhydrous, 99.8%), chlorobenzene (CB, 99.9%), acetonitrile (ACN, anhydrous, 99.8%) were purchased from Sigma Aldrich. Isopropyl alcohol (IPA, ≥99.9%) was purchased from Knowles. Lead iodide (PbI_2, >99.99%) were purchased from Advanced Election Technology, methylammonium chloride (MACl, >99.5%), methylammonium iodide (MAI, >99.5%), formamidinium iodide (FAI, >99.5%), 2,2′,7,7′-Tetrakis(N,N-di-pmethoxyphenylamino)-9,9′-spirobifluorene (spiro-OMeTAD, ≥99.5%), octylammonium iodide (OAI, >99.5%), 4-tert-butylpyridine (tBP, >96%), lithium bis(trifluoromethanesulphonyl)imide (Li-TFSI, >99%) were purchased from Xi'an Polymer Light Technology Corporation.

1,4-Bis(methyl)cyclohexaneammonium iodide ($BCMAI_2$) was synthesized by dissolving 1g of 1,4-Bis(aminomethyl)cyclohexane (99% Sigma) in 4 ml of ethanol absolute and reacting it slowly while stirring with 4ml of Hydroiodic acid (57 wt% in

water, Sigma). The reaction was carried out slowly while stirring to synthesize 1,4-Bis(methyl)cyclohexaneammonium iodide. In order to control the reaction rate and suppress the formation of by-products, the reaction was carried out in an ice bath at 0°C or lower. After the slow addition of acid, the precipitation was left for 20 minutes. After evaporation on a vacuum rotary evaporator for half an hour, the precipitate was filtered, then washed three times with diethyl ether and recrystallized twice with absolute ethanol. A white powder is obtained after drying for 6 hours in an oven at 40 ℃.

Solar cell fabrication

Rubbing the indium tin oxide (ITO) conductive glass with detergent to remove large impurities on the surface, and then use deionized water, isooctane and ethanol to clean the ITO conductive glass sheet with ultrasonic waves for 20 min, respectively. The ITO was dried under nitrogen flow and treated under UV ozone for 30 min to produce a hydrophilic surface. The SnO_2 precursor colloid was removed and deionized water was added until diluted to 2.5 wt%. The diluted SnO_2 colloids were coated on ITO substrates by spinning at 3000 rpm for 30 s and annealed at 150 °C for 30 min in an atmosphere of 30-40% humidity.

Perovskite active layers of $(FAPbI_3)_{0.97}(MAPbCl_3)_{0.03}$ were continuously fabricated using a two-step deposition method in a glove box filled with N_2. The lead iodide precursor solution was prepared by dissolving 691.5 mg of lead iodide and different concentrations of $BCMAI_2$ in 1 ml of DMF: DMSO (9:1) solvent, and the solution was heated and stirred at 70 °C for 6 h. The perovskite precursor solution was prepared by dissolving FAI: MAI: MACl in 1 ml IPA at a ratio of 90 mg FAI, 9 mg MACl and 6.4 mg MAI, and stirring at room temperature for 12 h. The lead iodide precursor solution containing $BCMAI_2$ was spin-coated on the ITO/SnO_2 substrate at 1500 rpm for 30 s and annealed at 70 °C for 15 s in a nitrogen-filled glove box. Then, the FAI: MAI: MACl mixed solution was spin-coated on the lead iodide film at 1500 rpm for 30 s. Then, the ITO substrates with deposited perovskite films were transfered from the glove box to room temperature atmosphere (30-40% humidity) and annealed

at 150 °C for 15 min. Dissolve 3 mg of OAI in 1ml of IPA and stir for 6 h to prepare the OAI solution. Simultaneously, mix 72.3 mg of spiro-OMeTAD, 28.8 μl of tBP, and 17.5 μl of Li-TFSI solution (520 mg Li-TFSI in 1 ml ACN) with 1 ml of CB and stir at room temperature for 6 h to prepare the hole transport layer solution. The OAI solution was spin-coated on top of the perovskite film at 5000 rpm in a glove box for 30 s and annealed at 100 °C for 5 min. After that, the spiro-OMeTAD solution was spin-coated on the perovskite film at 3000 rpm for 40 s in a glove box. After the preparation, the semi-finished device was transferred to a vacuum chamber to deposit 100 nm Ag at a base pressure of 6×10^{-4} Pa.

Materials and device characterization

PbI_2 and perovskite films were characterized by scanning electron microscopy (SEM) using ZEISS EV0 MA15. X-ray diffraction (XRD) patterns of PbI_2 films with or without $BCMAI_2$ addition were obtained using DX-2700, with Cu Kα radiation at 40 kV and 30 mA. XRD patterns of perovskite films were performed using Bruker AXS D8 Advance with Cu Kα radiation at 40 kV and 40 mA. X-ray photoelectron spectroscopy (XPS) measurements of PbI_2 and perovskite films were carried out by KRATOS XSAM800 with a monochromatic Al Kα X-ray source (hν = 1486.6 eV, 180 W). The XPS in-depth profiling measurements of perovskite films were conducted using Thermo Scientific with a monochromatic Al Kα X-ray source. Absorption spectra were measured by UV2600 of SHIMADZU. Steady-state photoluminescence (PL) and time-resolved PL (TRPL) were measured using FLS-980 Edinburgh instrument. I-V measurements and maximum power point tracking (MPPT) were obtained using Keithley B2901A source meter. AAAA solar simulator (SS-F5-3A, Enli Technology Co., Ltd.) was used to provide simulated sunlight. PSCs were measured in reverse scan (1.3 →-0.2 V, step size 0.1 V $s^{-1)}$ with AM1.5 G spectrum, and the intensity of the solar simulator was calibrated to 100 mW cm^{-2} using a silicon reference photodiode. The working area of PSCs was adjusted by the mask to 0.105 cm^2. Kelvin probe force microscopy (KPFM, KEYSIGHT Technologies 7500) was used to characterize the

surface root-mean-square (RMS) roughness and contact potential difference (CPD) of PbI_2 and perovskite films in tapping mode. Grazing-incidence X-ray diffraction (GIXRD) spectra were recorded by a PANalytical Empyrean (Netherlands). Dynamic light scattering (DLS) was performed by Anton paar litesizer 500. Ultraviolet Photoelectron Spectroscopy (UPS) was performed by PHI 5000 VersaProbe III with He I source (21.22 eV) under an applied negative bias of 9.0 V. Transmission electron microscope (TEM) was performed by Talos 200s (Thermo Fisher). The space-charge-limited current (SCLC) results were acquired using a Keithley B2901A source meter.

First-principles density functional theory (DFT) calculations were performed using the VASP software package with projector augmented-wave (PAW) electron structure. All surface and interface calculations were conducted with a plane-wave energy cutoff of 500 eV and a single Γ k-point. The exchange-correlation interactions were treated using the generalized gradient approximation of the Perdew-Burke-Ernzerhof (PBE) parametrization, with Grimme's D3 correction included to handle van der Waals interactions. The atomic force threshold in the structure relaxation process was 0.05 eV/Å, and the energy convergence threshold in all calculations was 1×10^{-4} eV. For surface terminated with either 2×2×2 FAI or PbI_2 of $FAPbI_3$ (a=6.43Å b=6.27 c=6.36) was utilized for adsorption calculations, where each surface slab was modeled with two layers of FAI/PbI_2. For 2D/3D perovskite heterojunctions consist of a 2D monolayer perovskite and a three-dimensional 2×2×2 $FAPbI_3$ supercell slab. The top one layers or the one layers near the interface were allowed to relax, while the other layers were fixed to their bulk positions. a vacuum with a thickness of no less than 15 Å was employed for all slab calculations. VASPKIT and VESTA were used for partial computational data preprocessing and structure picture output, respectively.

The total passivation energy (ΔE_{Tot}) is calculated following:

$$\Delta E = E_{Tot} - E_{Slab} - E_{Mol}$$

where E_{Tot} is the total energy of the passivation perovskite system, E_{Slab} is the total energy of the perovskite slab of FAI or PbI_2, and E_{Mol} is the energy of a single salt molecule.

The binding energy of the heterojunction is calculated by the following formula:

$$\Delta E = E_H - E_{2D} - E_{3D}$$

Where E_H is the energy of the heterojunction, E_{2D} is the energy of the isolated 2D part of the heterojunction, and E_{3D} is the energy of the isolated 3D part of the heterojunction.

The formation energies of 2D perovskite is calculated following:

$$\Delta E = E_{2D} - E_{Salt} - E_{PbI}$$

Where E_{2D} is of the energy if 2D perovskite, E_{Salt} is the energy of a single salt molecule ($BCMAI_2$), E_{PbI} is the energy of a bulk crystal structure PbI.

Statistical analysis

If no special processing method is mentioned in the following description, all data were processed using Origin software (Origin 2021 .lnk). The processing method involved importing the data of the X and Y axes into the software and selecting the desired plot type (scatter plot, scatter line plot, line plot) based on requirements.

In this case, the normalized slope plot of the lattice expansion coefficient in GIXRD (Grazing Incidence X-Ray Diffraction) was obtained using formula $d = \frac{n\lambda}{2\sin\theta}$ to calculate the interplanar spacing d. A scatter plot was created in Origin, and the software's built-in analysis tools were used to perform linear regression, resulting in the final outcome.

To open the raw data in Origin, simply click on "Import Single ASCII" in the toolbar or go to File → Import → Single ASCII to import the data. Then, use the following formulas to calculate C and $1/C^2$:

$$C = -\frac{1}{wZ''} = -\frac{1}{2\pi f Z''}$$

where f represents frequency.

Add two new columns in Origin labeled F and G. Select the F column, right-click, and choose "Set Column Values." Enter the formula to obtain the capacitance (C) data. Similarly, you can obtain the $1/C^2$ data. To plot the Mott-Schottky curve, select columns A and G, and plot the corresponding data points. The resulting plot should resemble the figure shown below.

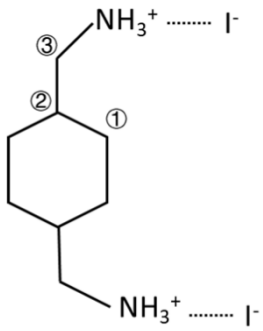

Figure S1. The structural formula of $BCMAI_2$.

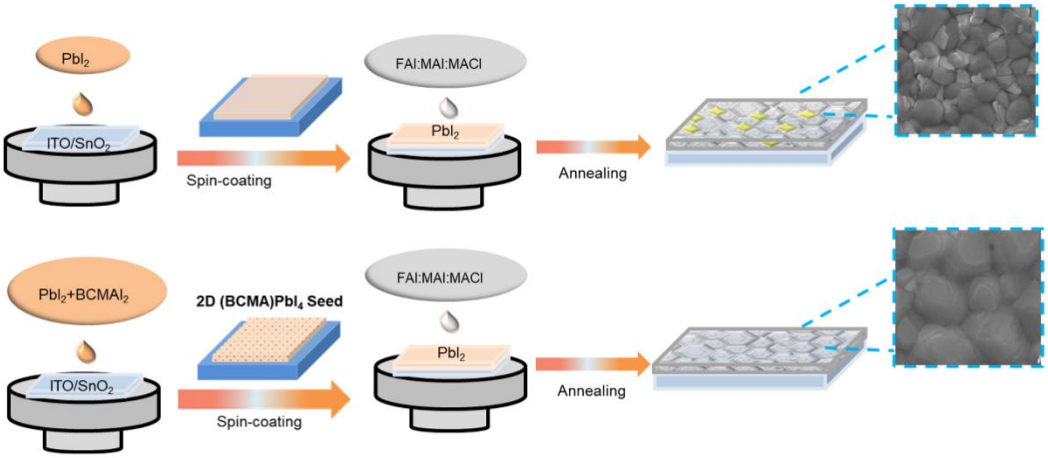

Figure S2. The process of preparing perovskite films by control and BISR method.

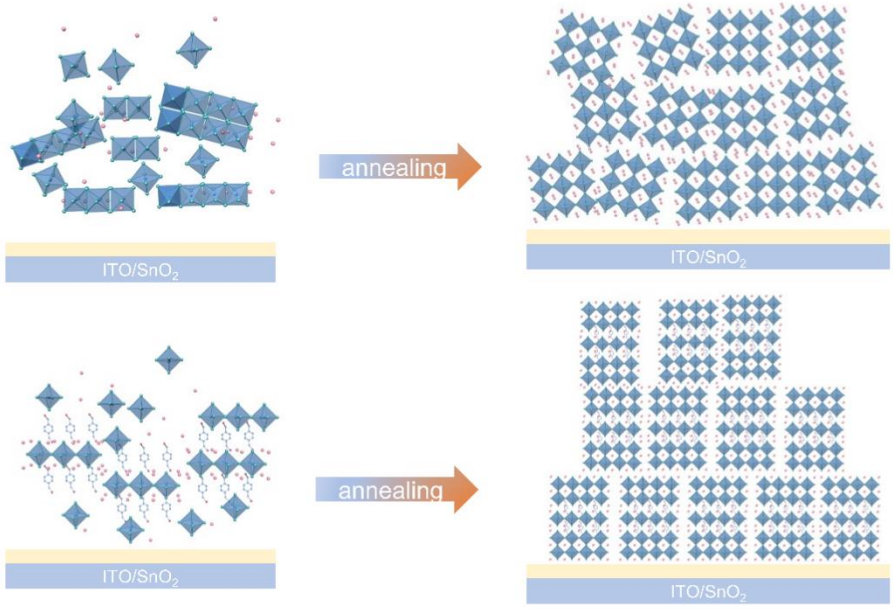

Figure S3. PVK growth mechanism of control and BISR method during annealing.

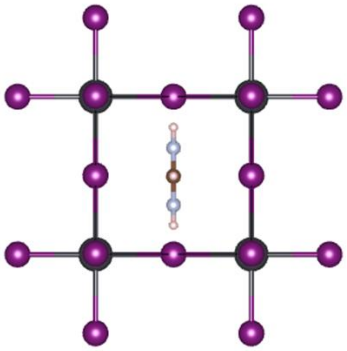

Figure S4. The DFT calculation result diagram of $FAPbI_3$ with binding energy of -1.71 eV

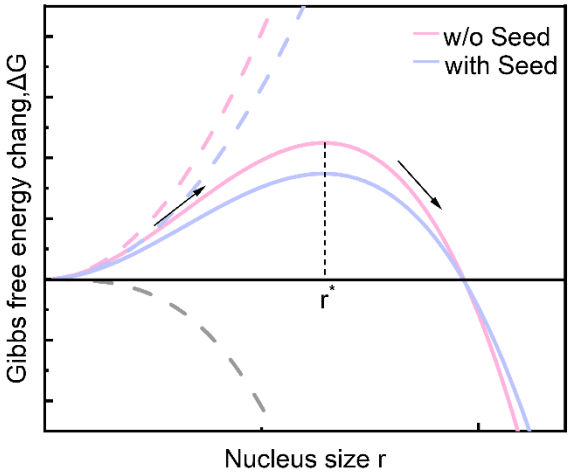

Figure S5. Schematic diagram of the Gibbs free energy of crystal growth process.

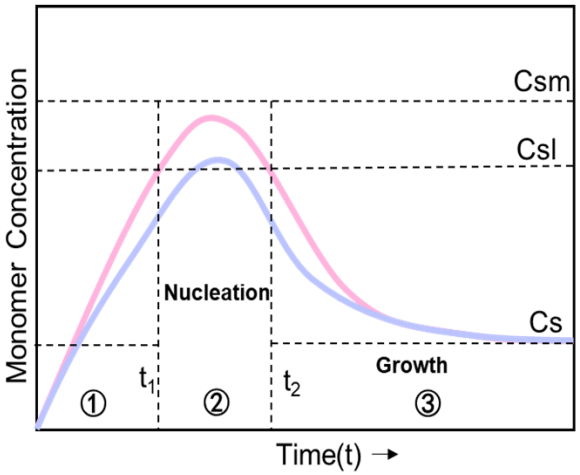

Figure S6. Lamer Model diagram.

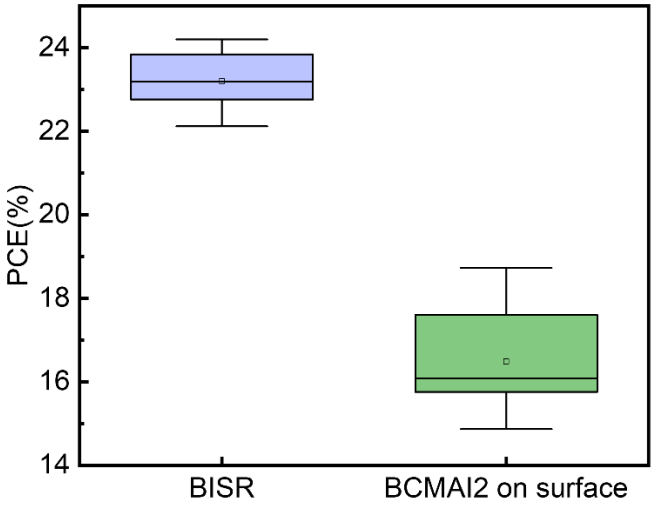
PCE(%)
24
22
20
18
16
14
BISR
BCMAI2 on surface

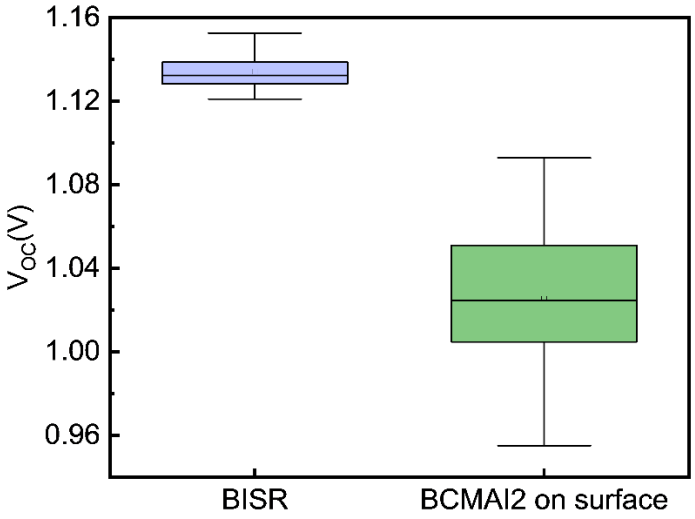
V_{OC}(V)
1.16
1.12
1.08
1.04
1.00
0.96
BISR
BCMAI2 on surface

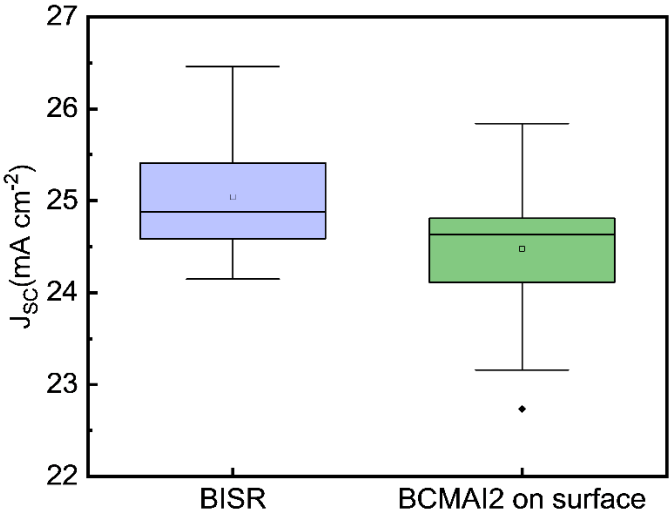
J_{SC}(mA cm^{-2})
27
26
25
24
23
22
BISR
BCMAI2 on surface

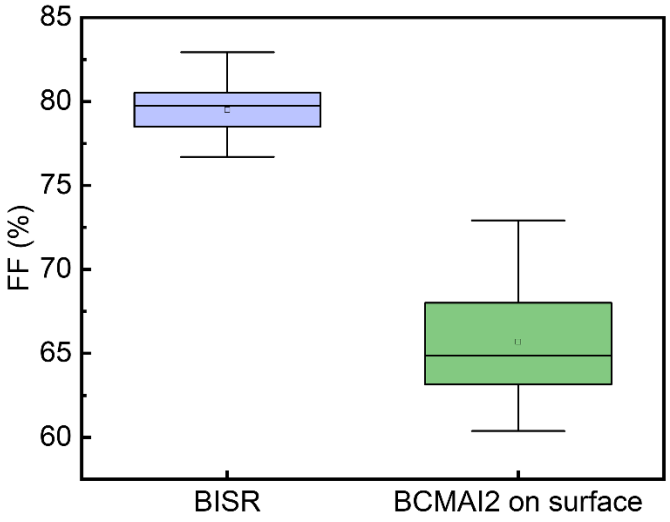

Figure S7. Statistical chart of BISR and $BCMAI_2$ spined on PVK surface based PSCs.

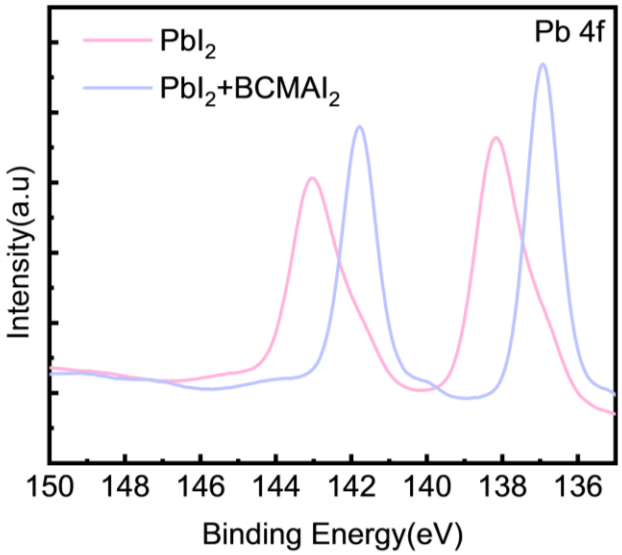

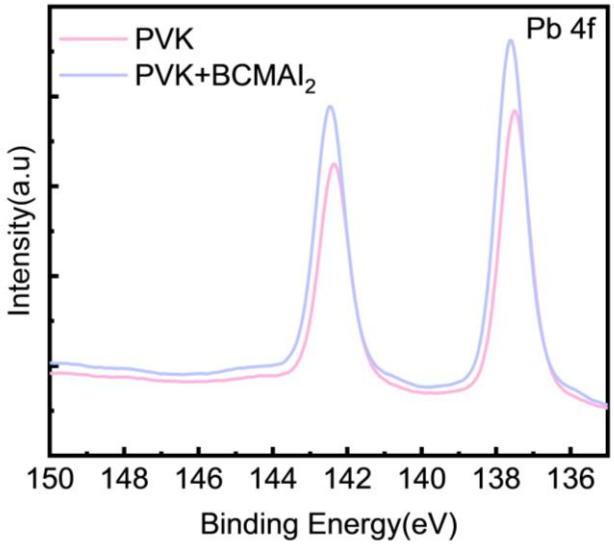

Figure S8. XPS of PbI_2 and PVK films on Pb 4f orbit.

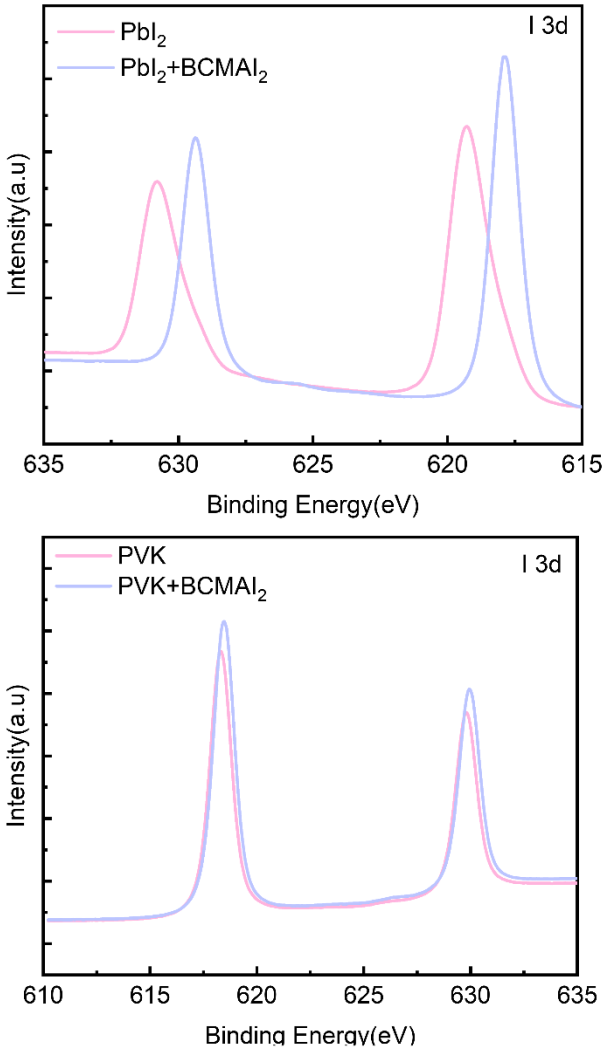

Figure S9. XPS of PbI_2 and PVK films on I 3d orbit.

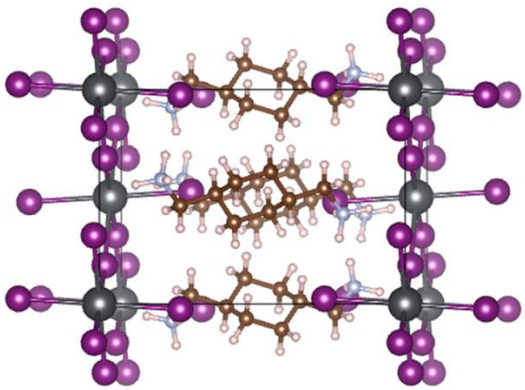

Figure S10: The DFT calculation of 2D (n=1) result, d-spacing=12.24 Å.

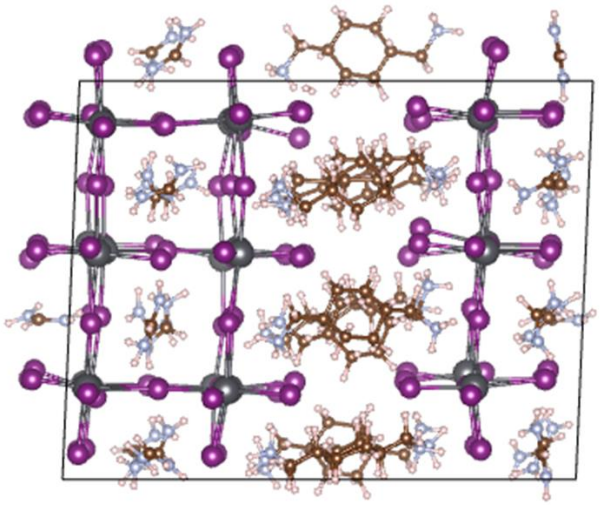

Figure S11: The DFT calculation of 2D (n=3) result, d-spacing=11.2 Å.

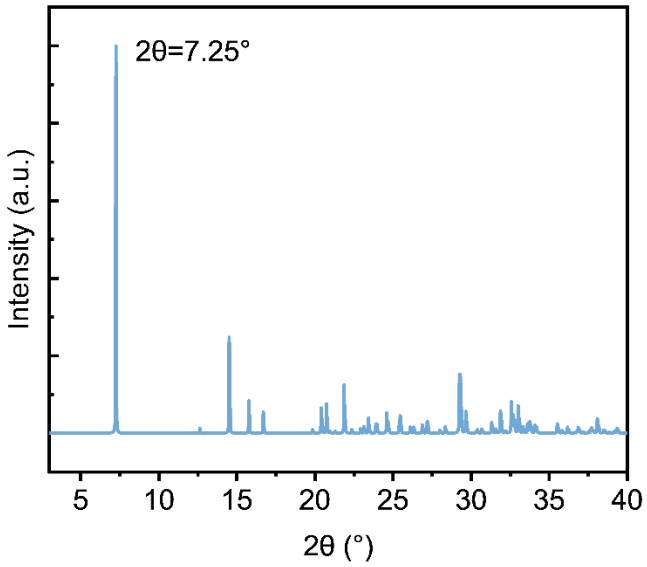

Figure S12. XRD of 2D PVK by DFT calculation.

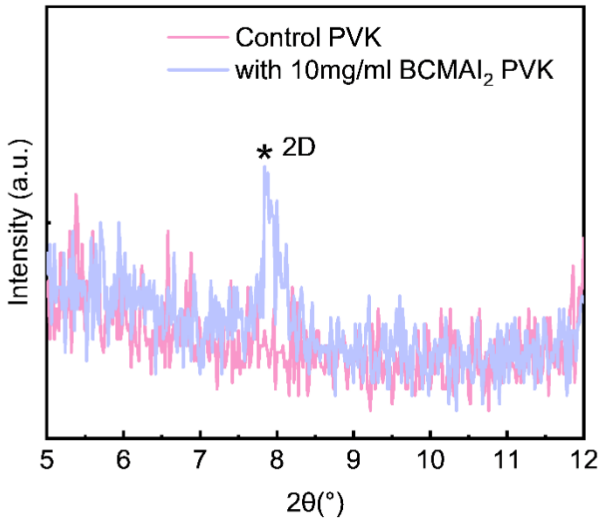

Figure S13. XRD of control and with 10mg/ml $BCMAI_2$ PVK, *(2θ=7.84°).

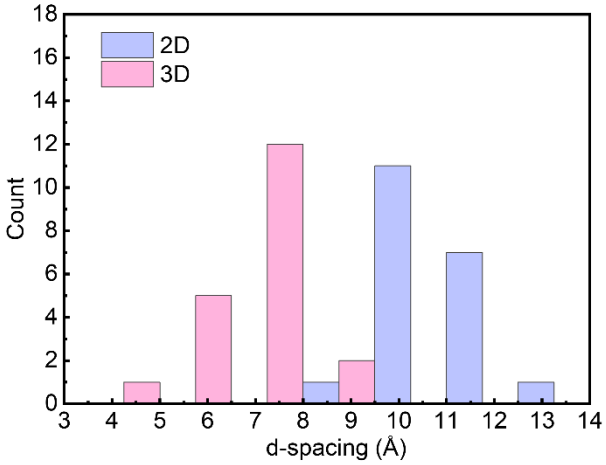

Figure S14. TEM of 2D and 3D crystal d-spacing statistics, each group corresponds to 20 samples.

Table S1. Fitted parameters of TRPL decay curves of control and target films stacked with or without ETL.

	A_1	A_2	τ_1(ns)	τ_2(ns)
Control(with)	1.63	98.37	74.81	334.23
Target(with)	7.08	92.92	76.03	205.73
Control(w/o)	5944.11	1230.57	146.58	300.66
Target(w/o)	651.66	651.67	512.09	625.89

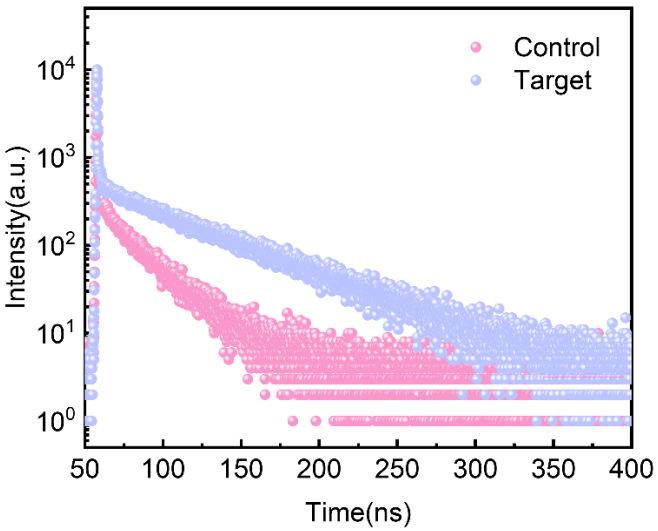

Figure S15. The TRPL of PVK on glass shows that the calculated T_{AVE} values for control and target are 191.94 ns and 574.12 ns.

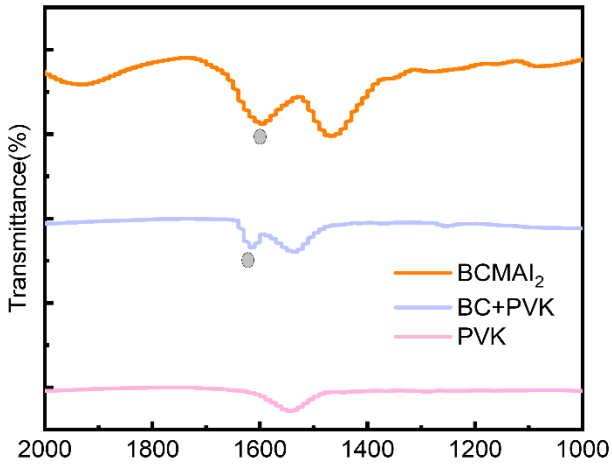

Figure S16. Fourier Transform infrared spectroscopy characterization graph.

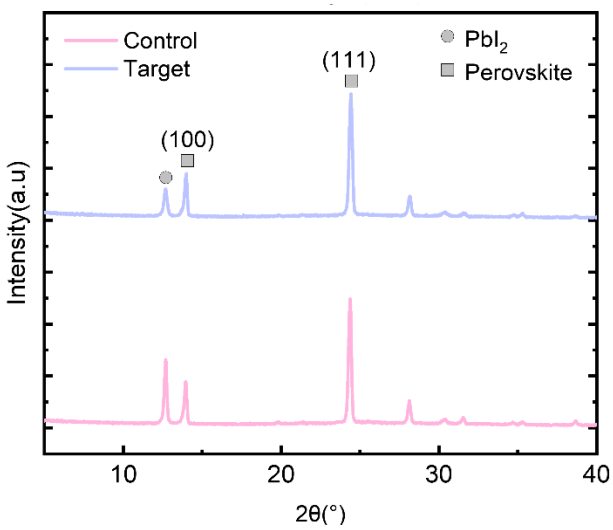

Figure S17. XRD of control and target films.

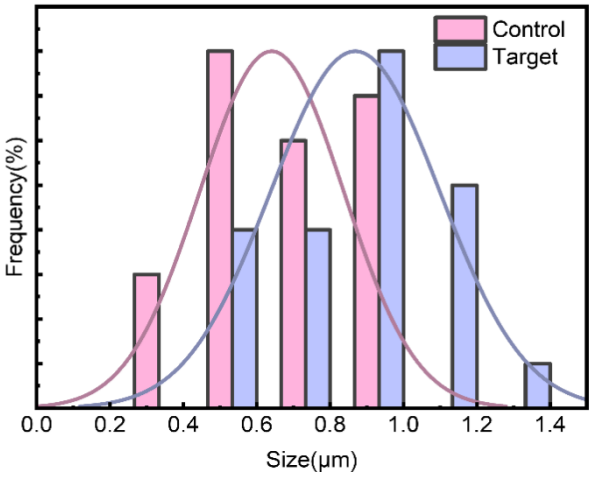

Figure S18. Surface grain size statistic of PVK films.

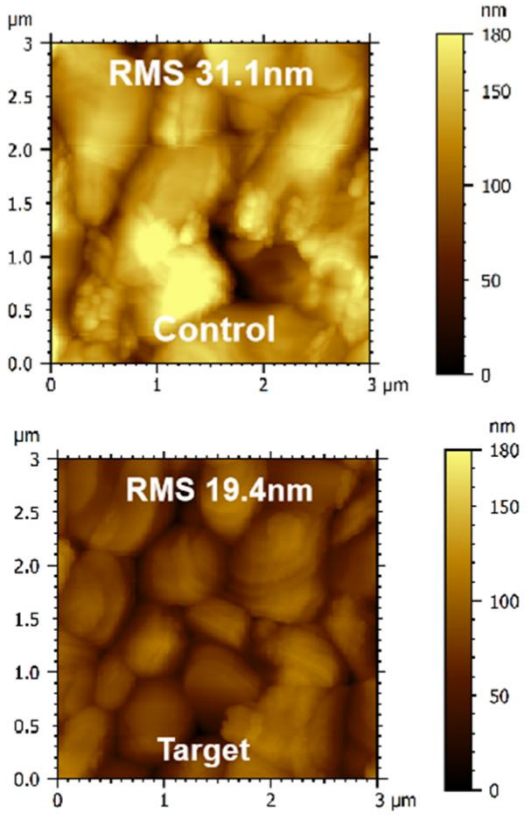

Figure S19. AFM of control and target PVK films.

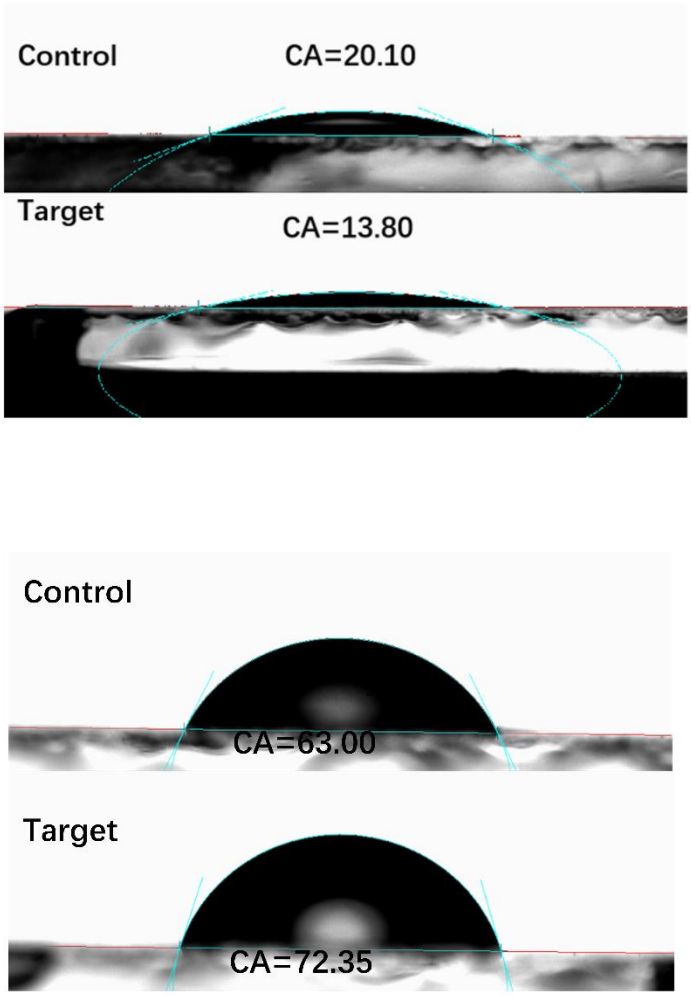

Figure S20. Contact angle of IPA solvent on PbI_2 film and water on PVK film surface.

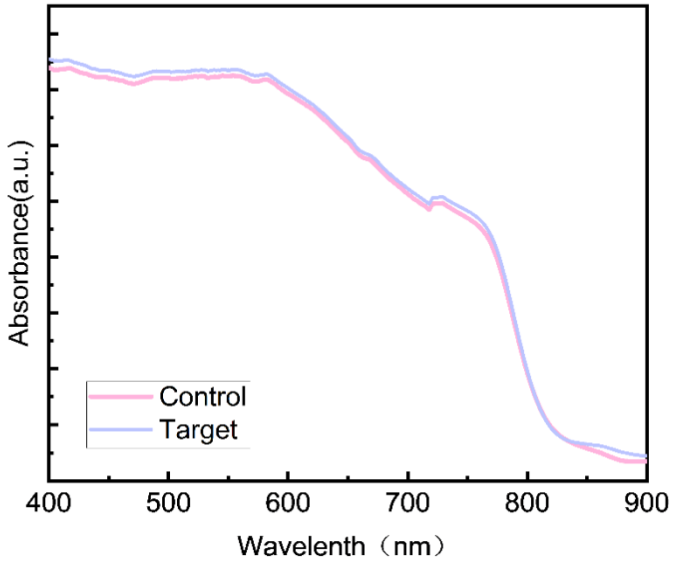

Figure S21. Ultraviolet-visible curves of control and target PVK films.

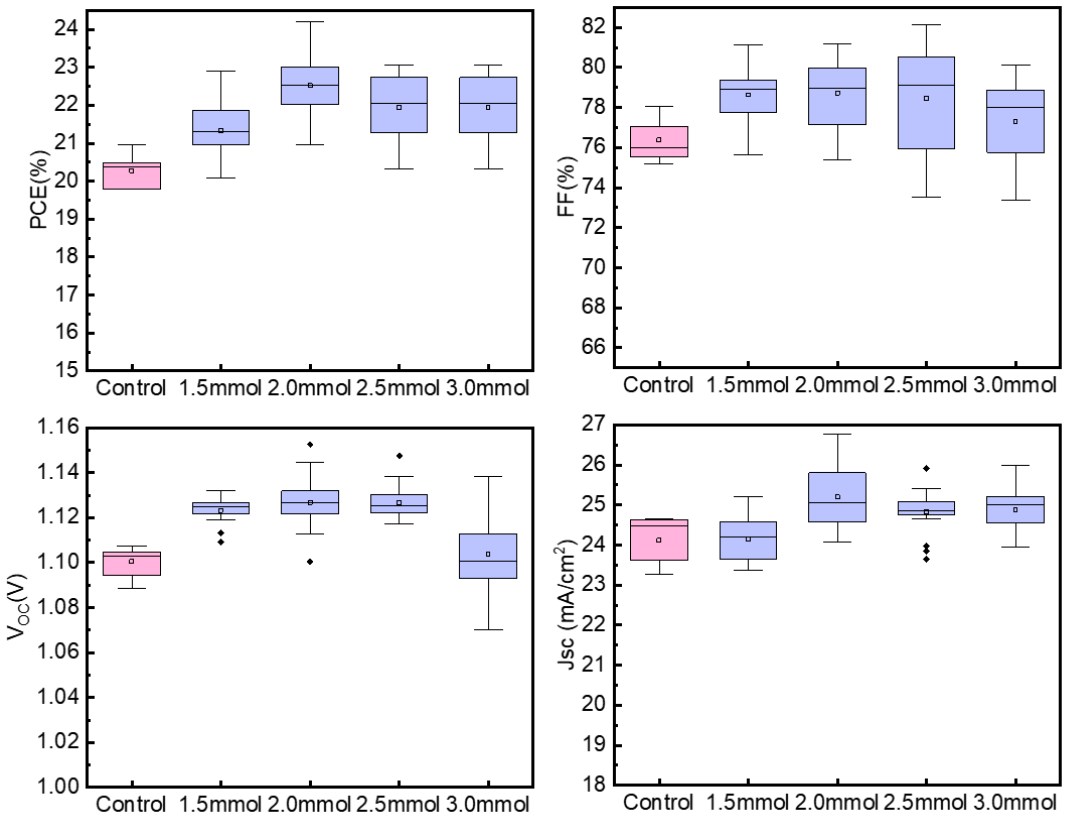

Figure S22. The PSCs performance corresponding to different concentrations of $BCMAI_2$.

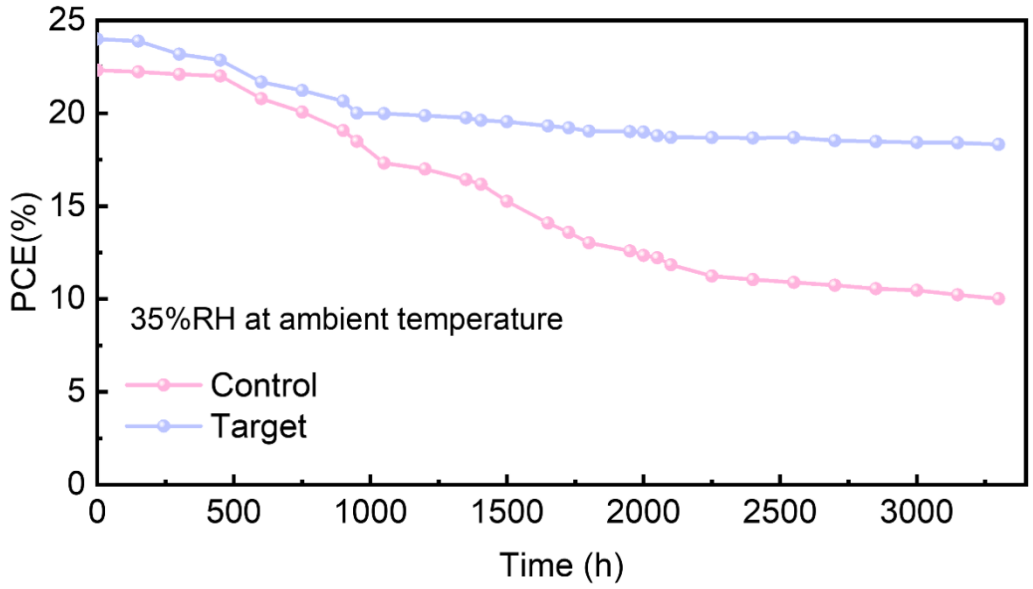

Figure S23. Stability tracking test of unpackaged control and target PSCs at 35%RH room temperature.

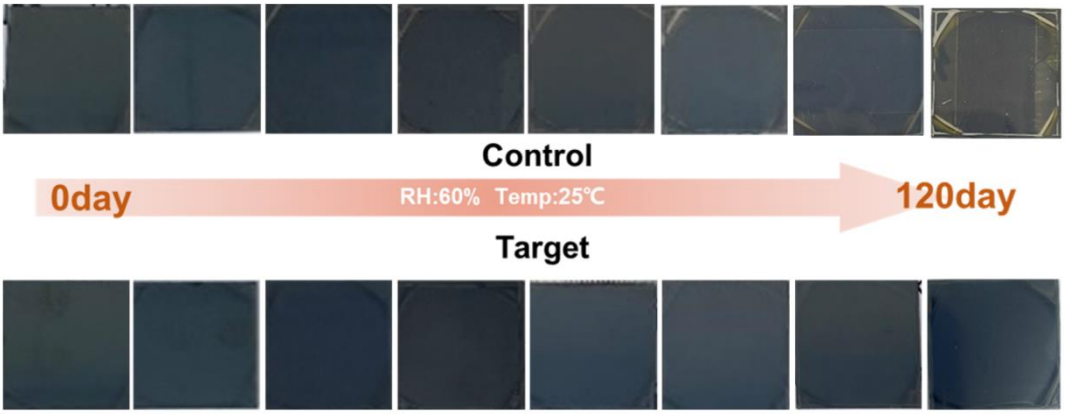

Figure S24. The images of continuous 120-days film evolution tracking for control and target film under conditions of 60% humidity and 25°C temperature.